ACS Photonics

Article

pubs.acs.org/journal/apchd5

Low-Loss Optical Waveguide and Highly Polarized Emission in a Uniaxially Oriented Molecular Crystal Based on 9,10-Distyrylanthracene Derivatives

Jinlong Chen, Suqian Ma, Jibo Zhang, Bao Li, Bin Xu,* and Wenjing Tian*

State Key Laboratory of Supramolecular Structure and Materials, Jilin Unversity, Changchun 130012, China

Supporting Information

ABSTRACT: A uniaxially oriented crystal based on 9,10-bis(2,2-di-*p*-tolylvinyl)anthracene (BDTVA) with an excellent waveguide and polarization performance has been prepared. The low loss coefficient (2.75 cm^{-1}) and the high polarization contrast (0.72) may result from the uniaxially oriented packing and layer-by-layer molecular structure in the BDTVA crystal. Moreover, amplified spontaneous emission is observed from the BDTVA crystal with a low threshold of 265 $\mu J/cm^2$, and the gain coefficient is 52 cm^{-1} at the peak wavelength of 509 nm. These features indicate that the BDTVA crystal may be potentially applied in the field of optical waveguides and organic solid-state lasers.

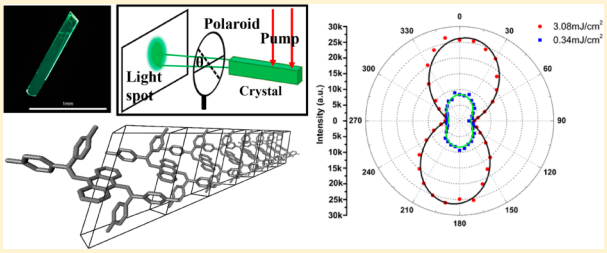

KEYWORDS: *optical waveguide, polarized emission, uniaxially oriented crystal, amplified spontaneous emission*

Organic single crystals have attracted intense attention for their distinct properties, such as high thermal stability, highly ordered structure, and preferential molecular orientation within the crystal lattice.[1−3] Optical waveguides and solid-state lasers based on organic single crystals are under intensive studies.[4−9] The performance of these devices is affected by the waveguide and polarized properties of the organic single crystal. For an organic single crystal, the optoelectronic properties not only depend on the luminophor but also depend significantly on the intermolecular interactions and molecular orientation.[10,11] An organic crystal with bidirectional molecular packing usually hinders the uniaxial polarization of the emission light,[12,13] while uniaxially oriented molecular crystals, in which the molecules are arranged in the same conformation and orientation, may possess excellent waveguide and highly polarized light emission performance, because the same molecular conformation and orientation within the crystal lattice will result in highly anisotropic refractive indices and direct the propagation of the emitting light in the preferential direction.[14,15] Over the past decades, only a few works on uniaxially oriented molecular crystals have been reported,[1,16−19] because it is difficult to make the organic molecules pack in the same orientation due to the multiple conformations of organic molecules and the various interactions in the crystals.[16] Ma and co-workers reported three uniaxially oriented molecular crystals: BCPEB,[17] CNDPASDB,[16] and CN-DPDSB.[1] BCPEB and CNDPASDB crystals showed outstanding amplified spontaneous emission (ASE) and polarized properties with the polarized ratio of 20 and 4.0 and threshold values of 360 and 305 $\mu J/cm^{-2}$, respectively. The CNDPASDB crystal showed efficient two-photon pumped up-conversion lasing with high polarization contrast.[18,19] The CN-DPDSB crystal possessed well-balanced bipolar carrier-transport characteristics and optically pumped laser properties.[1] Therefore, it will be of great importance to develop new uniaxially oriented organic single crystals with low-loss optical waveguide and highly polarized performance by adjusting the molecular packing structure for potential practical applications.

Herein, we present a new 9,10-distyrylanthracene derivative, BDTVA (Figure 1a), by introducing four methyl substituents to

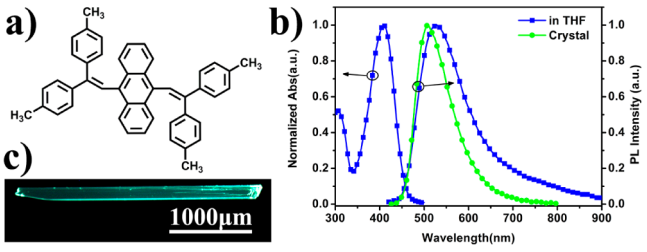

Figure 1. (a) Structure of BDTVA. (b) UV−vis and PL spectra of BDTVA in tetrahydrofuran (THF) and crystals. (c) Crystal photo under UV light.

the BDPVA molecule, which has been reported in our previous work on the fascinating optoelectronic properties.[20] BDTVA crystals show excellent waveguide and polarized light emission performance. The study on the BDTVA crystal structure reveals that the BDTVA crystal is a uniaxially oriented molecular crystal, which can lead to highly anisotropic refractive indices and direct the propagation of the emitted light in the

Received: November 19, 2014
Published: January 9, 2015

DOI: 10.1021/ph5004384
ACS Photonics 2015, 2, 313−318

preferential direction.[14] This is the main reason for the low-loss waveguide and highly polarized emission of the BDTVA crystal. The wide-angle X-ray diffraction experiment revealed the layer-by-layer structure in the BDTVA crystal, which may also contribute to the self-waveguided propagation of the fluorescent emission. Besides, ASE is also observed from the BDTVA crystal with a low threshold of 265 μJ/cm^2 per pulse, and the gain coefficient at the peak wavelength of 509 nm is 52 cm^{-1}.

RESULTS AND DISCUSSION

BDTVA was simply synthesized by the Wittig−Horner reaction according to our previous work.[20−22] The synthesis route and the characterized data are summarized in the Supporting Information (Scheme S1) and the Methods section.

The photophysical property of BDTVA was investigated by UV−vis absorption spectroscopy and photoluminescence (PL) spectroscopy in THF solution and in single crystals. As shown in Figure 1b, the absorption spectrum of BDTVA in THF solution possesses a main band around 408 nm, corresponding to the $\pi-\pi^*$ transition of the divinylanthracene moiety.[23] The emission spectrum of BDTVA in THF solution is broad and featureless, with the maximum emission at about 528 nm. In addition, BDTVA shows weak fluorescent emission in solution with a low fluorescent quantum efficiency (Φ_F) of 0.01 and short fluorescent lifetime (τ_{FL}) of 0.24 ns (Table S2). The reason is that the rotational and vibrational motions of peripheral tolyls can deplete the energy of the excited molecules through nonradiative deactivation, resulting in the low Φ_F and featureless broad emission.[24,25] However, BDTVA shows significantly enhanced fluorescent intensity when water is added into its THF solution, suggesting that it is AIE-active (Figure S1 and Table S1).[26−28]

The crystals of BDTVA are highly emissive under UV illumination. As shown in Figure 1b, the PL spectrum of the BDTVA crystal exhibits a strong green emission peaking at 507 nm and a blue shift compared to that of the THF solution, indicating that the conformation of BDTVA molecules in the single crystal may be more twisted than those in solutions.[20] Actually, the fluorescent quantum efficiency (Φ_F) of the BDTVA crystal is as high as 0.50, and the fluorescent lifetime (τ_{FL}) is as long as 1.96 ns (Figure S2 and Table S2), which are higher than that in THF solution. According to the equations reported by the previous work,[11,29] the radiative rate constant (k_r) and the nonradiative rate constant (k_{nr}) can be approximately estimated as listed in Table S2. k_r did not decrease in the crystal, while k_{nr} decreased nearly 1 order of magnitude in the crystals compared with that in THF solution, which means the nonradiative decay pathway was blocked in the crystal and the fluorescent efficiency of the BDTVA crystal increased significantly.[10] Interestingly, there was a notable spot of bright PL at the tip of the crystal, whereas the remaining surface showed only a relatively weak green emission (Figure 1c). This phenomenon revealed that the BDTVA crystal could absorb the excitation light and transport the PL emission toward the end of the crystal. Such localization of the out-coupling light at the end of each crystal was a typical characteristic of waveguide behavior.[30]

In order to characterize the waveguide performance of the BDTVA crystal, we measured the loss coefficient of the waveguides by the spatially resolved PL spectra via the local excitation of the crystal body (Figure 2a). Figure 2b shows the PL intensity at the end of a single crystal under different

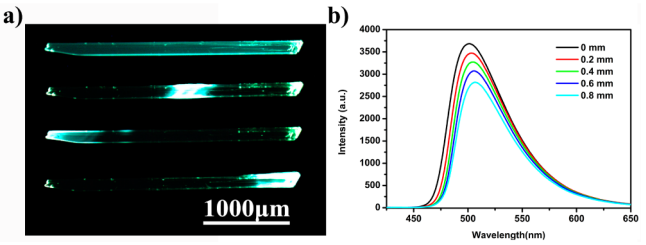

Figure 2. (a) FL microscopy image collected upon excitation of the identical crystal at three different positions. (b) Spatially resolved PL spectra of the emission that is out-coupled at the tip of a single crystal from a distance of 0−0.8 mm from the tip.

excitation positions. The spectral intensity and profiles of the excited light did not change substantially with the position along the BDTVA crystal. However, the emission intensity at the tip decreased almost exponentially with increasing the propagation distance. The emission intensity from the pump stripe I_0 is kept constant, and the emission intensity from the tip of the sample decrease as $I = I_0 \exp(-\alpha x)$, where x is the distance between the crystal tip and the location of optical excitation along the crystal body and α is the loss coefficient. By fitting the intensity data at different wavelengths of the PL spectra as a function of x using the above equation, the curve of the loss coefficient versus wavelength could be obtained, as shown in Figure S3. The loss coefficient decreases gradually from the short wavelength to the long wavelength, until it stays nearly constant. The loss coefficient is 2.75 cm^{-1} at 509 nm, which is significantly lower than many other organic single crystals that have been reported.[17,31] In general, the loss coefficient is mainly affected by two factors. The first is the reabsorption during the propagation of the light along the crystal. In the region of short wavelength, the emission band overlaps with the absorption band of the BDTVA crystal (Figure S4), which is harmful for the light propagation and results in a high loss coefficient. In the region of long wavelength, the emission and absorption spectra of the BDTVA crystal are well separated (Figure S4), which is beneficial to propagating light in the crystal and results in a low loss coefficient. The second is Rayleigh scattering resulting from the defects in the crystal and the roughness of the crystal surface. Therefore, the low loss coefficient for the BDTVA crystal should be attributed to the well-separated absorption and emission bands (Figure S4), which decrease the reabsorption together with the smooth surface (RMS = 0.126, Figure S5) to reduce the light scattering.

During the investigation of the waveguide performance of the BDTVA crystal, we found that the emission light from the crystal tip was polarized. In other words, BDTVA crystals also possess polarization properties. Figure 3a shows the intensity of the out-coupling light emitted from the tip of the BDTVA crystal with respect to the polarization orientation angle at the excitation wavelength of λ_{ex} = 355 nm under the pumping laser energy of 3.08 and 0.34 mJ/cm^2. As expected, the emission intensity showed very strong dependence on the polarization and the distribution function for the linear polarization (Figure 3) in the crystal. It could be well fitted by a cosine quadratic function ($\cos^2 \theta$), which is a characterization of the polarized emission from the uniaxially aligned chromophores.[18] The parameter θ refers to the angle between the horizontal direction of the crystal and the polarization direction of the linear polarizer placed before the CCD detector, as shown in the inset

DOI: 10.1021/ph5004384
ACS Photonics 2015, 2, 313−318

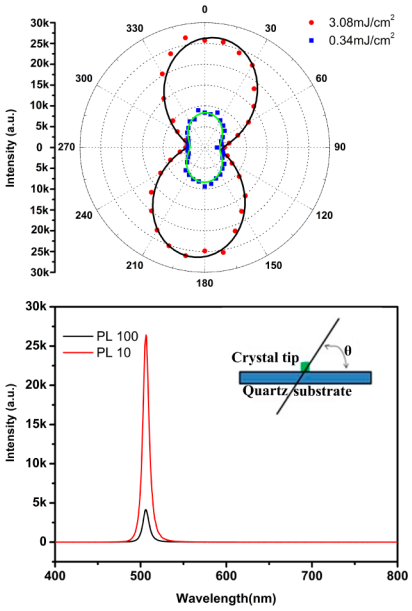

Figure 3. (a) PL intensity of the crystal with respect to the polarization of the pump laser at excitation wavelength of λ_{ex} = 355 nm (pump intensity is 0.34 mJ/cm^2 and 3.08 mJ/cm^2). (b) Fluorescence spectrum excited at two different polarizations, θ = 100° and θ = 10° (pump intensity is 3.08 mJ/cm^2).

of Figure 3b. The maximum of the out-coupling emission intensity occurred at polarization angles about 10° and 190°. It means that the BDTVA crystal was most efficiently coupled with the laser electrical field in this orientation. The minimum intensity of the PL spectrum appeared at the polarization angles of about 100° and 280°, which are approximately perpendicular to the polarization direction of the maximum emission intensity. The present study clearly revealed that the polarization of out-coupling emission light seemed to be independent of the energy of the pumping laser, suggesting that the polarization of output is due to the intrinsic molecular packing. The PL intensity of the out-coupling emission with an oblique angle about 10° and 100° against the surface of ribbon-like BDTVA crystals under the pumping laser energy of 3.08 mJ/cm^2 is shown in Figure 3b. The emission dichroic ratio, i.e., the ratio of the emission intensities between the maximum ($\theta \approx$ 10° or 190°) and the minimum ($\theta \approx$ 100° or 280°), could reach 6.21, which is higher than that of the organic crystal with the uniaxial orientation packing reported previously.[16] The polarization contrast C is as high as 0.72 according to the equation $C = (I_{max} - I_{min})/(I_{max} + I_{min})$, where I_{max} and I_{min} are the maximal and minimal polarization components of the PL emission, respectively. The high polarization contrast of the BDTVA crystal means the emission from the tip of the BDTVA crystal is nearly perfectly linearly polarized.

Generally, polarized emission is a direct consequence of the highly ordered alignment of π-conjugated molecules due to the intrinsic anisotropy of their electronic structure.[3] To investigate the origin of the low-loss waveguide and high polarization properties, large single BDTVA crystals were prepared by physical vapor deposition, and the stacking mode was analyzed by single-crystal X-ray diffraction.

The BDTVA crystals belong to the triclinic system, space group $P\bar{1}$. Each unit cell consists of one crystallographically independent molecule (Figure 4a and b). Similar to other DSA derivatives, the molecular conformation of BDTVA in the

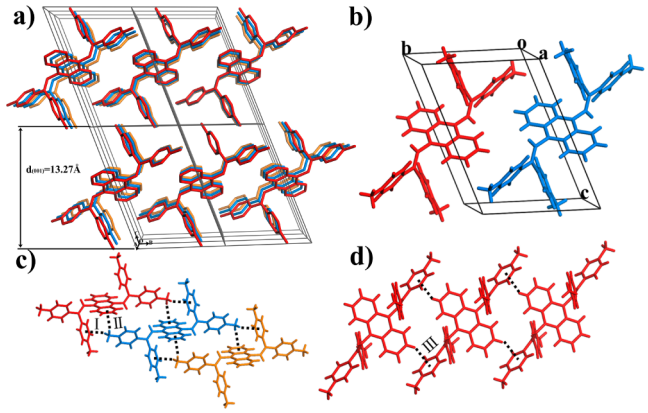

Figure 4. (a) Uniaxially oriented alignment of BDTVA molecules in the crystal. (b) Unit cell structure of the BDTVA crystal. (c) CH/π interaction I and interaction II. (d) CH/π interaction III.

crystal is remarkably twisted due to the steric hindrance arising from the hydrogen atoms on vinyl and anthracene.[2,20,32] The torsional angle between the double bond and central anthracene is 112.16° ($\theta_{(1,2,3,4)}$), and the torsional angles between the double bond and two adjacent phenyl rings are 38.37° ($\theta_{(3,4,5,6)}$) and 133.13° ($\theta_{(3,4,7,8)}$), respectively (Figure S6 and Table S3). These torsional angles are all larger than those in the BDPVA crystal,[20] suggesting that the introduction of methyl substituents to the BDPVA molecule results in the more twisted molecular conformation. As a result, the molecules in the BDTVA crystal are far away from each other by the distance between the central anthracenes of the adjacent molecules of 6.457 Å, indicating that there is no face-to-face $\pi-\pi$ interactions between the adjacent molecules.[33]

The most intriguing structural feature of the BDTVA crystal is the uniaxially oriented packing. As shown in Figure 4a, all the molecules in the BDTVA crystal are arranged in the same conformation and orientation. The uniaxially oriented packing is the most conducive to the optical properties such as the light propagation and polarized performance because the emission from the same orientation single molecule can easily interact in a certain phase with respect to the optical field.[14−16] According to a meticulous analysis of the crystal structure of BDTVA, we found there are three different types of CH$-\pi$ interactions influencing BDTVA molecules to assemble themselves into the absolutely uniaxial orientation. As shown in Figure 4c and d, the interaction distance and the angle of C−H$-\pi$ center for interaction I are 3.008 Å and 141.03°, and for interaction II they are 3.012 Å and 141.52°, while for interaction III they are 2.944 Å and 142.08°, respectively. The CH$-\pi$ interactions attach the molecular clusters and drive the uniform orientation of BDTVA molecules along the axis (Figure 4a). When BDTVA molecules aggregate, the twisted conformation of the molecule protects the center divinyl-anthracene from forming a face-to-face $\pi-\pi$ interaction, which is detrimental for the fluorescence. The multiple weak intermolecular interactions induced the molecules to form the uniaxially oriented packing crystal and also markedly inhibited the torsional and vibrational motions,[20] which result in the BDTVA crystal possessing high fluorescent quantum efficiency and outstanding optical properties.

We also investigated the relationship between the crystalline lattice and the ribbon-like single crystal by the wide-angle X-ray diffraction. Figure S7 shows the wide-angle X-ray diffraction

DOI: 10.1021/ph5004384
ACS Photonics 2015, 2, 313−318

pattern of the ribbon-like BDTVA single crystal. Since the surface of the ribbon-like single crystal was parallel to the substrate, the diffraction pattern revealed the layer-by-layer structure. The first strong diffraction peak at 6.68°corresponds to the diffraction spacing of ~13.23 Å according to the Bragg equation, which is almost equal to the d_{001} (13.27 Å), suggesting the layer-by-layer structure in the crystal is parallel to the *ac*-plane. Such ordered structure and the regularly oriented molecules of the single crystal may contribute to the significant anisotropy of the optical properties, resulting in the outstanding waveguide and polarized light emission performance of the BDTVA crystal.

Generally, the excellent waveguide and polarized properties are beneficial to the amplified spontaneous emission, so we investigated the ASE properties of the BDTVA crystal. The crystal was optically pumped with a third harmonic (355 nm, 10 ns) of a Q-switched Nd:YAG laser at a repetition rate of 10 Hz after being focused into a stripe by a cylindrical lens. The pump laser energy was adjusted by the calibrated neutral density filters.

Figure 5a shows the dependence of the emission spectrum for a BDTVA crystal on the excitation intensity. At a weak

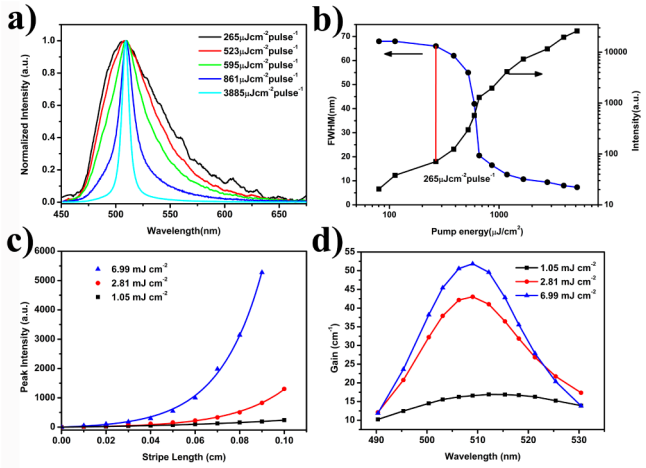

Figure 5. (a) PL spectra of a BDTVA crystal as a function of the pump laser energy. (b) Dependence of the peak intensity and fwhm of the emission spectra on the pump laser energy. (c) Peak intensity of the emission as a function of pump stripe length under different pump energies and (d) the net gain coefficients as a function of wavelength.

excitation density of 265 μJ/cm^2 per pulse, a broad PL spectrum with a full width at half-maximum (fwhm) of ~68 nm appeared. With the increase of the excitation density to 3885 μJ/cm^2 per pulse, the emission is amplified into gain-narrowed bands with a fwhm of ~8 nm. Figure 5b shows the peak intensity and fwhm of the PL spectra as a function of the excitation density. A significant nonlinear increase in emission intensity and a rapid decrease in fwhm were observed as the optical excitation intensity increased, confirming the occurrence of ASE in the BDTVA crystal.[34] The onset of the spectral narrowing, which is usually known as the phenomenological threshold, is determined to be 265 μJ/cm^2 pulse^{-1}.

To verify ASE and get the gain coefficient, the optical gain measurement was carried out by the variable pump stripe method. Figure 5c shows the output intensity at the peak (509 nm) of the emission spectrum as a function of pump stripe length at three different pump intensities. By fitting the intensity data at different wavelengths of PL spectra as a function of pump stripe length by the equation shown in the Methods section, the net gain coefficient at different wavelengths can be obtained and are shown in Figure 5d. At a pump intensity of 1.05 mJ/cm^2 pulse^{-1}, the net gain coefficient at 509 nm is 17 cm^{-1}, while the net gain coefficient at 509 nm is as high as 52 cm^{-1} at a pump intensity of 6.99 mJ/cm^2 pulse^{-1}, and the output intensity increased by more than 2 orders of magnitude as the excitation length was increased. At higher pump intensities, the net gain was higher and the output intensity increased exponentially at excitation lengths of less than 1 mm. The perfect agreement of the data with the equation in the Methods section is strong evidence for the amplification of the spontaneous emission by the stimulated emission.[34]

CONCLUSIONS

In summary, a uniaxially oriented crystal based on 9,10-bis(2,2-dip-tolylvinyl)anthracene (BDTVA) with excellent waveguide and polarization performance has been prepared. The loss coefficient and the polarization contrast are 2.75 cm^{-1} and 0.72, respectively, which may be ascribed to the uniaxially oriented packing as well as the layer-by-layer structure of the BDTVA crystal. In addition, ASE is observed from the BDTVA crystal with a low threshold (265 μJ/cm^2 per pulse), and the gain coefficient at the peak wavelength of 509 nm is 52 cm^{-1}. These features indicate that the BDTVA crystal may be potentially applied in the field of optical waveguides and organic solid-state lasers.

METHODS

Materials and Characterization Techniques. Anthracene (99%) was purchased from J&K Chemical Co. (China), 4,4′-dimethylbenzophenone (>99%) was purchased from TCI Shanghai Chemical Co. (China), potassium *tert*-butoxide was purchased from Acros Organic Co. (Belgium), and all other reagents were purchased as analytical grade from either Tianjin Fuyu Co. (China) or Beijing Chemical Reagent Co. (China) and used without further purification, unless otherwise noted. Anhydrous tetrahydrofuran (THF) was dried by distillation from sodium/benzophenone. ^{1}H NMR spectra were recorded on a Bruker AVANVE 500 MHz spectrometer with chloroform-*d* as solvent and tetramethylsilane (TMS) as internal standard. The time-of-flight mass spectra were recorded using a Kratos MALDI-TOF mass system.

Synthesis of BDTVA. Compound **2**, tetraethylanthracene-9,10-diylbis(methylene) diphosphonate (0.5 g, 1.04 mmol), and 4,4′-dimethylbenzophenone (0.879 g, 4.18 mmol) were dissolved in THF (70 mL) under nitrogen. *t*-BuOK (1.0 g, 8.93 mmol) in THF (40 mL) was added to the solution, which was kept at room temperature. Then the solution was kept at 50 °C and stirred for 12 h. The resultant precipitate was washed successively with MeOH and filtered off to give the compound as a yellow powder (41.8% yield). ^{1}H NMR (500 MHz, $CDCl_3$, δ): 2.05 (s, 3H; CH_3), 2.13 (s, 3H; CH_3), 2.43 (s, 6H; CH_3), 6.61 (d, J = 8.0 Hz; 2H, Ar), 6.64 (d, J = 7.9 Hz; 2H, Ar), 6.70 (d, J = 8.1 Hz; 2H, Ar), 6.78 (d, J = 8.0 Hz; 2H, Ar), 7.21−7.25 (m, 4H; Ar), 7.27−7.30 (m, 4H; Ar), 7.43−7.49 (m, 5H; Ar, CH═C), 7.52 (s, 1H; CH═C), 8.14−8.23 (m, 4H; Ar) VMALDI/TOF MS: calcd for $C_{46}H_{38}$ 590.30, found 590.12.

As the intermediate products, compound **1**, 9,10-bis-(dichloromethyl)anthracene, and compound **2**, tetraethyl

DOI: 10.1021/ph5004384
ACS Photonics 2015, 2, 313−318

anthracene-9,10-diylbis(methylene)diphosphonate, were synthesized according to the procedure reported.[20−22]

Photophysical Properties of BDTVA Measurements. UV−vis absorption spectra were recorded on a Shimadzu UV-3100 spectrophotometer. Photoluminescence spectra were collected on a Shimadzu RF-5301PC spectrophotometer and Maya 2000Pro optical fiber spectrophotometer. Crystalline-state PL efficiencies were measured with an integrating sphere (C-701, Labsphere Inc. America), with a 405 nm Ocean Optics LLS-LED as the excitation source, and the laser was introduced into the sphere through the optical fiber. The fluorescence microscopy images were obtained on an Olympus BX51 fluorescence microscope.

BDTVA Crystal Structural Analysis. Large single BDTVA crystals were prepared by physical vapor deposition. The crystal diffraction data were collected on a Rigaku RAXISPRID diffractometer using the ω-scan mode with graphite-monochromated Mo Kα radiation. The wide-angle X-ray diffraction patterns were recorded by a Rigaku SmartLab X-ray diffractometer with Cu Kα radiation (λ = 1.5418 Å). Atomic force micrographs were recorded under ambient conditions using a SPA300 (SEIKO) operating in tapping mode. CCDC 999808 contains the supplementary crystallographic data for this paper. These data can be obtained free of charge from the Cambridge Crystallographic Centre via www.ccdc.cam.ac.uk/data_request/cif.

ASE Measurements. The single crystal was placed on a quartz substrate and irradiated by the third harmonic (355 nm) of a Nd:YAG (yttrium−aluminum−garnet) laser at a repetition rate of 10 Hz and pulse duration of about 10 ns. The laser beam was focused into a stripe by using a cylindrical lens and a slit. The edge emission of the crystals was detected using an optical fiber connected with a Maya2000Pro optical fiber spectrophotometer. All the measurements were carried out at room temperature under ambient conditions. The peak intensity increased exponentially with increasing pump stripe length, which satisfies the following equation:

$$I(\lambda) = \frac{A(\lambda)I_p}{g(\lambda)}(e^{g(\lambda)l} - 1)$$

where A is a constant related to the cross section for the spontaneous emission, I_p is the pump intensity, g is the net gain coefficient, and l is the length of the pumped stripe.

■ ASSOCIATED CONTENT

Supporting Information

A scheme showing the synthesis route of BDTVA; figures showing the Abs and PL spectra, fluorescence lifetime, selected dihedral angles, XRD, and AFM image of BDTVA; tables showing the optical properties, selected dihedral angles, and crystal data of BDTVA. This material is available free of charge via the Internet at http://pubs.acs.org.

■ AUTHOR INFORMATION

Corresponding Authors

*E-mail: xubin@jlu.edu.cn.
*E-mail: wjtian@jlu.edu.cn.

Notes

The authors declare no competing financial interest.

■ ACKNOWLEDGMENTS

This work was supported by the 973 Program (2013CB834702), the Natural Science Foundation of China (51373063, 21204027, 21221063), Program for Chang Jiang Scholars and Innovative Research Team in University (IRT101713018), the Research Fund for the Doctoral Program of Higher Education of China (20120061120016), and the Graduate Innovation Fund of Jilin University (2014013).

■ REFERENCES

(1) Wang, H.; Li, F.; Ravia, I.; Gao, B. R.; Li, Y. P.; Medvedev, V.; Sun, H. B.; Tessler, N.; Ma, Y. G. Cyano-Substituted Oligo(p-phenylene vinylene) Single Crystals: A Promising Laser Material. *Adv. Funct. Mater.* **2011**, *21*, 3770−3777.

(2) Chen, J. L.; Ma, S. Q.; Xu, B.; Zhang, J. B.; Dong, Y. J.; Tian, W. J. Molecular Crystals Based on 9,10-Distyrylanthracene Derivatives with High Solid State Fluorescence Efficiency and Uniaxial Orientation Induced by Supramolecular Interactions. *Chin. Sci. Bull.* **2013**, *58*, 2747−2752.

(3) Mizuno, H.; Haku, U.; Marutani, Y.; Ishizumi, A.; Yanagi, H.; Sasaki, F.; Hotta, S. Single Crystals of 5,5′-Bis(4′-methoxybiphenyl-4-yl)-2,2′-bithiophene for Organic Laser Media. *Adv. Mater.* **2012**, *24*, 5744−5749.

(4) Yanagi, H.; Morikawa, T. Self-waveguided Blue Light Emission in P-sexiphenyl Crystals Epitaxially Grown by Mask-Shadowing Vapor Deposition. *Appl. Phys. Lett.* **1999**, *75*, 187−189.

(5) Zhang, C.; Zhao, Y. S.; Yao, J. N. Optical Waveguides at Micro/Nanoscale Based on Functional Small Organic Molecules. *Phys. Chem. Chem. Phys.* **2011**, *13*, 9060−9073.

(6) Heng, L. P.; Wang, X. Y.; Tian, D. L.; Zhai, J.; Tang, B. Z.; Jiang, L. Optical Waveguides Based on Single-Crystalline Organic Micro-Tiles. *Adv. Mater.* **2010**, *22*, 4716−4720.

(7) McGehee, M. D.; Heeger, A. J. Semiconducting (Conjugated) Polymers as Materials for Solid-State Lasers. *Adv. Mater.* **2000**, *12*, 1655−1668.

(8) Ichikawa, M.; Hibino, R.; Inoue, M.; Haritani, T.; Hotta, S.; Araki, K.; Koyama, T.; Taniguchi, Y. Laser Oscillation in Monolithic Molecular Single Crystals. *Adv. Mater.* **2005**, *17*, 2073−2077.

(9) Shimizu, K.; Mori, Y.; Hotta, S. Laser Oscillation from Hexagonal Crystals of a Thiophene/Phenylene Co-oligomer. *J. Appl. Phys.* **2006**, *99*, 063505.

(10) Gierschner, J.; Ehni, M.; Egelhaaf, H. J.; Medina, B. M.; Beljonne, D.; Benmansour, H.; Bazan, G. C. Solid-state Optical Properties of Linear Polyconjugated Molecules: π-Stack Contra Herringbone. *J. Chem. Phys.* **2005**, *123*, 144914.

(11) Yoon, S. J.; Chung, J. W.; Gierschner, J.; Kim, K. S.; Choi, M. G.; Kim, D.; Park, S. Y. Multistimuli Two-Color Luminescence Switching via Different Slip-Stacking of Highly Fluorescent Molecular Sheets. *J. Am. Chem. Soc.* **2010**, *132*, 13675−13683.

(12) Yamada, Y.; Yanagi, H. Polarized Blue Light-Emission from Epitaxially Oriented Bis(phenyloxazolyl)benzene Crystals. *Appl. Phys. Lett.* **2000**, *76*, 3406−3408.

(13) Bauer, C.; Urbasch, G.; Giessen, H.; Meisel, A.; Nothofer, H. G.; Neher, D.; Scherf, U.; Mahrt, R. F. Polarized Photoluminescence and Spectral Narrowing in an Oriented Polyfluorene Thin Film. *ChemPhysChem* **2000**, *1*, 142−146.

(14) Varghese, S.; Yoon, S. J.; Calzado, E. M.; Casado, S.; Boi, P. G.; García, M. A. D.; Resel, R.; Fischer, R.; Medina, B. M.; Wannemacher, R.; Park, S. Y.; Gierschner, J. Stimulated Resonance Raman Scattering and Laser Oscillation in Highly Emissive Distyrylbenzene-Based Molecular Crystals. *Adv. Mater.* **2012**, *24*, 6473−6478.

(15) Yamao, T.; Okuda, Y.; Makino, Y.; Hotta, S. Dispersion of the Refractive Indices of Thiophene/Phenylene Co-oligomer Single Crystal. *J. Appl. Phys.* **2011**, *110*, 053113.

(16) Li, Y. P.; Shen, F. Z.; Wang, H.; He, F.; Xie, Z. Q.; Zhang, H. Y.; Wang, Z. M.; Liu, L. L.; Li, F.; Ma, Y. G. Supramolecular Network Conducting the Formation of Uniaxially Oriented Molecular Crystal of Cyano Substituted Oligo(p-phenylene vinylene) and Its Amplified

DOI: 10.1021/ph5004384
ACS Photonics 2015, 2, 313−318

Spontaneous Emission (ASE) Behavior. *Chem. Mater.* **2008**, *20*, 7312−7318.
(17) Xu, Y. X.; Zhang, H. Y.; Li, F.; Shen, F. Z.; Wang, H.; Li, X. J.; Yu, Y.; Ma, Y. G. Supramolecular Interaction-Induced Self-Assembly of Organic Molecules into Ultra-long Tubular Crystals with Wave Guiding and Amplified Spontaneous Emission. *J. Mater. Chem.* **2012**, *22*, 1592−1597.
(18) Fang, H. H.; Yang, J.; Ding, R.; Chen, Q. D.; Wang, L.; Xia, H.; Feng, J.; Ma, Y. G.; Sun, H. B. Polarization Dependent Two-Photon Properties in an Organic Crystal. *Appl. Phys. Lett.* **2010**, *97*, 101101.
(19) Fang, H. H.; Chen, D. Q.; Yang, J.; Xia, H.; Ma, Y. G.; Wang, H. Y.; Sun, H. B. Two-Photon Excited Highly Polarized and Directional Upconversion Emission from Slab Organic Crystals. *Opt. Lett.* **2010**, *35*, 441−443.
(20) Zhang, J. B.; Xu, B.; Chen, J. L.; Ma, S. Q.; Dong, Y. J.; Wang, L. J.; Li, B.; Ye, L.; Tian, W. J. An Organic Luminescent Molecule: What Will Happen When the "Butterflies" Come Together? *Adv. Mater.* **2014**, *26*, 739−745.
(21) Dong, Y. J.; Xu, B.; Zhang, J. B.; Tian, X.; Wang, L. J.; Chen, J. L.; Lv, H. G.; Wen, S. P.; Li, B.; Ye, L.; Zou, B.; Tian, W. J. Piezochromic Luminescence Based on the Molecular Aggregation of 9,10-Bis((E)-2-(pyrid-2-yl)vinyl)anthracene. *Angew. Chem., Int. Ed.* **2012**, *51*, 10782−10785.
(22) Zhang, J. B.; Chen, J. L.; Xu, B.; Wang, L. J.; Ma, S. Q.; Dong, Y. J.; Li, B.; Ye, L.; Tian, W. J. Remarkable Fluorescence Change Based on the Protonation−Deprotonation Control in Organic Crystals. *Chem. Commun.* **2013**, *49*, 3878−3880.
(23) He, J. T.; Xu, B.; Chen, F. P.; Xia, H. J.; Li, K. P.; Ye, L.; Tian, W. J. Aggregation-Induced Emission in the Crystals of 9,10-Distyrylanthracene Derivatives: The Essential Role of Restricted Intramolecular Torsion. *J. Phys. Chem. C* **2009**, *113*, 9892−9899.
(24) Xu, B.; He, J. T.; Dong, Y. J.; Chen, F. P.; Yu, W. L.; Tian, W. J. Aggregation Emission Properties and Self-Assembly of Conjugated Oligocarbazoles. *Chem. Commun.* **2011**, *47*, 6602−6604.
(25) Zhang, J. B.; Xu, B.; Chen, J. L.; Wang, L. J.; Tian, W. J. Oligo(phenothiazine)s: Twisted Intramolecular Charge Transfer and Aggregation-Induced Emission. *J. Phys. Chem. C* **2013**, *117*, 23117−23125.
(26) Chang, Z. F.; Jiang, Y. B.; He, B. R.; Chen, J.; Yang, Z. Y.; Lu, P.; Kwok, H. S.; Zhao, Z. J.; Qiu, H. Y.; Tang, B. Z. Aggregation-Enhanced Emission and Efficient Electroluminescence of Tetraphenylethene-Cored Luminogens. *Chem. Commun.* **2013**, *49*, 594−596.
(27) Li, H. Y.; Chi, Z. G.; Xu, B. J.; Zhang, X. Q.; Li, X. F.; Liu, S. W.; Zhang, Y.; Xu, J. R. Aggregation-Induced Emission Enhancement Compounds Containing Triphenylamine-anthrylenevinylene and Tetraphenylethene Moieties. *J. Mater. Chem.* **2011**, *21*, 3760−3767.
(28) Zhang, X. Q.; Chi, Z. G.; Xu, B. J.; Chen, C. J.; Zhou, X.; Zhang, Y.; Liu, S. W.; Xu, J. R. End-Group Effects of Piezofluorochromic Aggregation-Induced Enhanced Emission Compounds Containing Distyrylanthracene. *J. Mater. Chem.* **2012**, *22*, 18505−18513.
(29) Bernard, V. *Molecular Fluorescence Principles and Applications*; Wiley-VCH: Weinheim, Germany, 2002.
(30) Li, L.; Lu, H.; Yang, Z. Y.; Tong, L.; Bando, Y.; Golberg, D. Bandgap-Graded CdS_xSe_{1-x} Nanowires for High-Performance Field-Effect Transistors and Solar Cells. *Adv. Mater.* **2013**, *25*, 1109−1113.
(31) Luo, H. W. S.; Chen, J.; Liu, Z. T.; Zhang, C.; Cai, Z. X.; Chen, X.; Zhang, G. X.; Zhao, Y. S.; Decurtins, S.; Liu, S. X.; Zhang, D. Q. A Cruciform Electron Donor−Acceptor Semiconductor with Solid-State Red Emission: 1D/2D Optical Waveguides and Highly Sensitive/Selective Detection of H_2S Gas. *Adv. Funct. Mater.* **2014**, *24*, 4250−4258.
(32) Dong, Y. J.; Xu, B.; Zhang, J. B.; Lu, H. G.; Wen, S. P.; Chen, F. P.; He, J. T.; Li, B.; Ye, L.; Tian, W. J. Supramolecular Interactions Induced Fluorescent Organic Nanowires with High Quantum Yield Based on 9,10-Distyrylanthracene. *CrystEngComm* **2012**, *14*, 6593−6598.
(33) Shimizu, M.; Takeda, Y.; Higashi, M.; Hiyama, T. 1,4-Bis(alkenyl)-2,5-dipiperidinobenzenes: Minimal Fluorophores Exhibiting Highly Efficient Emission in the Solid State. *Angew. Chem., Int. Ed.* **2009**, *48*, 3653−3656.
(34) McGehee, M. D.; Gupta, R.; Veenstra, S.; Miller, E. K.; Díaz-García, M. A.; Heeger, A. J. Amplified Spontaneous Emission from Photopumped Films of a Conjugated Polymer. *Phys. Rev. B* **1998**, *58*, 7035−7039.

DOI: 10.1021/ph5004384
ACS Photonics 2015, 2, 313−318